Flavodiiron proteins act as safety valve for electrons in *Physcomitrella patens*

Caterina Gerotto[a,1], Alessandro Alboresi[a], Andrea Meneghesso[a], Martina Jokel[b], Marjaana Suorsa[b], Eva-Mari Aro[b], and Tomas Morosinotto[a,2]

[a]Department of Biology, University of Padova, 35121 Padova, Italy; and [b]Department of Biochemistry, Molecular Plant Biology, University of Turku, FI-20014 Turku, Finland

Edited by Pierre A. Joliot, Institut de Biologie Physico-Chimique, Paris, France, and approved September 2, 2016 (received for review April 27, 2016)

Photosynthetic organisms support cell metabolism by harvesting sunlight to fuel the photosynthetic electron transport. The flow of excitation energy and electrons in the photosynthetic apparatus needs to be continuously modulated to respond to dynamics of environmental conditions, and Flavodiiron (FLV) proteins are seminal components of this regulatory machinery in cyanobacteria. FLVs were lost during evolution by flowering plants, but are still present in nonvascular plants such as *Physcomitrella patens*. We generated *P. patens* mutants depleted in FLV proteins, showing their function as an electron sink downstream of photosystem I for the first seconds after a change in light intensity. *flv* knock-out plants showed impaired growth and photosystem I photoinhibition when exposed to fluctuating light, demonstrating FLV's biological role as a safety valve from excess electrons on illumination changes. The lack of FLVs was partially compensated for by an increased cyclic electron transport, suggesting that in flowering plants, the FLV's role was taken by other alternative electron routes.

photosynthesis | electron transport | photoprotection | plant evolution | mosses

Life on Earth depends on oxygenic photosynthesis, which enables plants, algae, and cyanobacteria to convert light into chemical energy. Sunlight powers the transfer of electrons from water to $NADP^+$ by the activity of two photosystems (PS), PSII and PSI, thus generating NADPH and ATP to sustain cell metabolism. Natural environmental conditions are highly variable, and sudden changes in irradiation can drastically affect the flow of excitation energy and electrons. At the same time, the ATP and NADPH consumption rate is also highly dynamic because of a continuous metabolic regulation (1–3). Photosynthetic organisms evolved several mechanisms to modulate the flow of excitation energy and electrons according to metabolic constraints, diverting/feeding electrons from/to the linear transport chain (3). These pathways modulate the ATP/NADPH ratio, as in the cyclic electron transport (CET) around PSI, where electrons are redirected from PSI to plastoquinone (PQ) or Cytb_6f (4), contributing to proton translocation and ATP synthesis, but not to NADPH formation (5–9).

In cyanobacteria, the Flavodiiron proteins (known as FLV) have been identified as an additional component of electron transport chain (10–12). FLV proteins are constituted by three distinct domains: a N-terminal β-lactamase-like domain, a flavodoxin-like domain, and a C-terminal NAD(P)H-flavin reductase-like domain. The former two domains are also found in FLV proteins from archaea and anaerobic bacteria, where they are involved in O_2 or NO reduction, whereas the latter is typical only of FLVs from oxygenic photosynthetic organisms (11–13). Recent studies showed that in cyanobacteria, the FLV1/FLV3 heterodimer catalyzes the light-dependent reduction of O_2 to water, using NADPH as electron donor (10, 11), protecting PSI from light stress (10). Another FLVs heterodimer, FLV2/FLV4, instead, has been shown to be active in photo-protection of PSII (14–16). FLVs also were found expressed in green algae as *Chlamydomonas reinhardtii* (17, 18), and corresponding genes are present in nonvascular plants (16) and in gymnosperms (19), but they were lost during evolution by flowering plants. Heterologous expression of FLV from the moss *Physcomitrella patens* in *Arabidopsis thaliana* recently showed that these proteins can be functional in flowering plants (19), suggesting their loss is not a result of structural reasons but, rather, a change in strategy for regulation of photosynthetic electron flow during land colonization that made FLV activity superfluous, or possibly even detrimental.

In this article, we generated *P. patens* mutants depleted in FLVA or FLVB proteins, showing that they are active as an electron sink downstream of PSI, and that their role is prominent in the first seconds after a sudden increase of light intensity, acting as a safety valve for electrons. When exposed to a fluctuating light regime, *flva* or *flvb* knock-out (KO) mutants have impaired growth and suffer from severe PSI photoinhibition. In mutant plants, FLV absence was partially compensated for by an enhanced cyclic electron flow, suggesting this as a likely mechanism that took the biological role of FLV in angiosperms.

Results

Depletion of Either FLVA or FLVB Affects the Accumulation of Both Isoforms in *Physcomitrella patens*. Two genes encoding the FLV proteins, named *FLVA* and *FLVB*, are found in the genome of the moss *P. patens* and show high similarity to cyanobacterial FLV1/FLV3 isoforms (*SI Appendix*, Fig. S1) (3, 11, 16). FLV biological function in *P. patens* was investigated by generating specific *flva* KO and *flvb* KO plants exploiting homologous recombination in the nuclear genome (20, 21) (*SI Appendix*, Fig. S2*A*).

Significance

Photosynthesis regulation is fundamental to responding to environmental dynamic changes and avoiding oxidative damage. These regulatory mechanisms were shaped during evolution from cyanobacteria to plants, as well as after the colonization of new habitats. Land colonization was a key phase in evolution with plants capable of adapting to drastically different conditions with respect to their aquatic ancestors. Valuable information on this adaptation can be obtained studying nonvascular plants, such as the moss *Physcomitrella patens*, that diverged from flowering plants early after land colonization. Here we show that in *P. patens*, Flavodiiron (FLV) proteins are acting as an electron sink to avoid photosynthetic electron transport chain over-reduction after any increase in illumination and are fundamental for protection under fluctuating light conditions.

Author contributions: C.G., E.-M.A., and T.M. designed research; C.G., A.A., A.M., M.J., and M.S. performed research; C.G., A.A., E.-M.A., and T.M. analyzed data; and C.G. and T.M. wrote the paper.

The authors declare no conflict of interest.

This article is a PNAS Direct Submission.

[1]Present address: Department of Biochemistry, Molecular Plant Biology, University of Turku, FI-20014 Turku, Finland.

[2]To whom correspondence should be addressed. Email: tomas.morosinotto@unipd.it.

This article contains supporting information online at www.pnas.org/lookup/suppl/doi:10.1073/pnas.1606685113/-/DCSupplemental.

For each genotype, at least four independent lines were isolated, and they all showed indistinguishable phenotypes (*SI Appendix*, Fig. S3). In all lines, we first verified the disruption of the target gene by the insertion of the resistance cassette (*SI Appendix*, Figs. S2*B* and S3*A*). RT-PCR showed that *FLVA* and *FLVB* transcripts were missing in *flva* KO and *flvb* KO lines, respectively (Fig. 1*A* and *SI Appendix*, Fig. S3), whereas they were both detectable in WT plants, demonstrating that the isolated clones were indeed genuine KO lines.

FLV proteins accumulation was evaluated afterward, using specific antibodies raised against *P. patens* FLVA or FLVB polypeptides. In both cases, a band was detectable in WT, but not in the *flva* KO and *flvb* KO lines (Fig. 1*B*). Even if the depletion of a single *flv* gene did not affect the RNA accumulation of the other *FLV* gene, the protein accumulation of FLVA and FLVB showed instead a strong mutual dependence (Fig. 1). This suggests that FLVA and FLVB form a heterodimer, as their cyanobacteria homologs (10), and that each monomer is not stably accumulated if expressed alone.

FLV Proteins Are a Major Electron Sink at the Onset of Light. When grown in control conditions, mutants depleted in FLV proteins showed no significant differences in growth, pigment content, or photosynthetic quantum yield with respect to WT (*SI Appendix*, Table S1), suggesting the mutation had no major effect on the accumulation of protein complexes of the photosynthetic apparatus. Photosynthetic electron transport rate (ETR) in the different genotypes was then measured using electrochromic shift, following the approach used in different organisms, including *P. patens* (refs. 22–26; see also *SI Appendix*, Fig. S4). In dark-acclimated WT plants, approximately 1 s after the light was switched on, ETR showed a peak, the intensity of which depended on the illumination intensity (*SI Appendix*, Fig. S5*A*). After this peak, ETR slowly and steadily increased during the illumination, consistent with the increased consumption rate of ATP and NADPH on the activation of the Calvin-Benson cycle (*SI Appendix*, Fig. S5*A*) (25). *flva* KO and *flvb* KO showed significantly reduced ETR compared with WT either with a mild irradiation (*SI Appendix*, Fig. S5*B*) or with saturating light (Fig. 2*A*), where the transient peak in ETR was completely absent. This difference, however, was only detectable for a few seconds after the onset of illumination, whereas later ETR was indistinguishable between the three genotypes, and they all reached the same value of ~ 60 e^-/s after 5 min of light treatment (Fig. 2*A*).

The same analyses were also performed in the presence of 3-(3,4-dichlorophenyl)-1,1-dimethylurea (DCMU), which inhibits PSII and therefore allows evaluating CET rate around PSI (22, 25) (Fig. 2*B*). In WT plants, CET is relatively low and stable at ~ 5 e^-/s, thus representing less than 10% of total electron transport (Fig. 2*B*), as reported in the literature for *P. patens* and other plant species (23, 25, 27). In contrast, *flva* KO and *flvb* KO plants showed a sustained cyclic electron transport activity for the first 10 s of illumination when it represents the major electron transport pathway

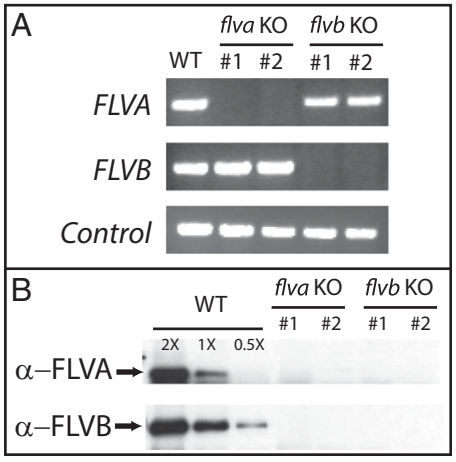

Fig. 1. Genotype characterization of *flva* KO and *flvb* KO lines. Effective homologous recombination with the insertion of the resistance cassette in *FLVA* or *FLVB* loci was first verified by PCR to prove the integration of resistance cassette in the expected position of the genome (*SI Appendix*, Fig. S2). (*A*) *FLVA* and *FLVB* gene expression was assessed by RT-PCR in WT and selected *flva KO* and *flvb* KO lines grown in control light. Amplification of *Actin* transcript is also reported as control. (*B*) Western blotting against *P. patens* FLVA and FLVB proteins. In each lane, 100 μg total proteins from CL-grown samples were loaded. In the case of WT, 0.5X and 2X indicates lanes loaded with 50 or 200 μg, respectively. WT and two independent lines for each *flva* KO and *flvb* KO mutants are reported, but additional independent lines were analyzed with indistinguishable results (*SI Appendix*, Fig. S3).

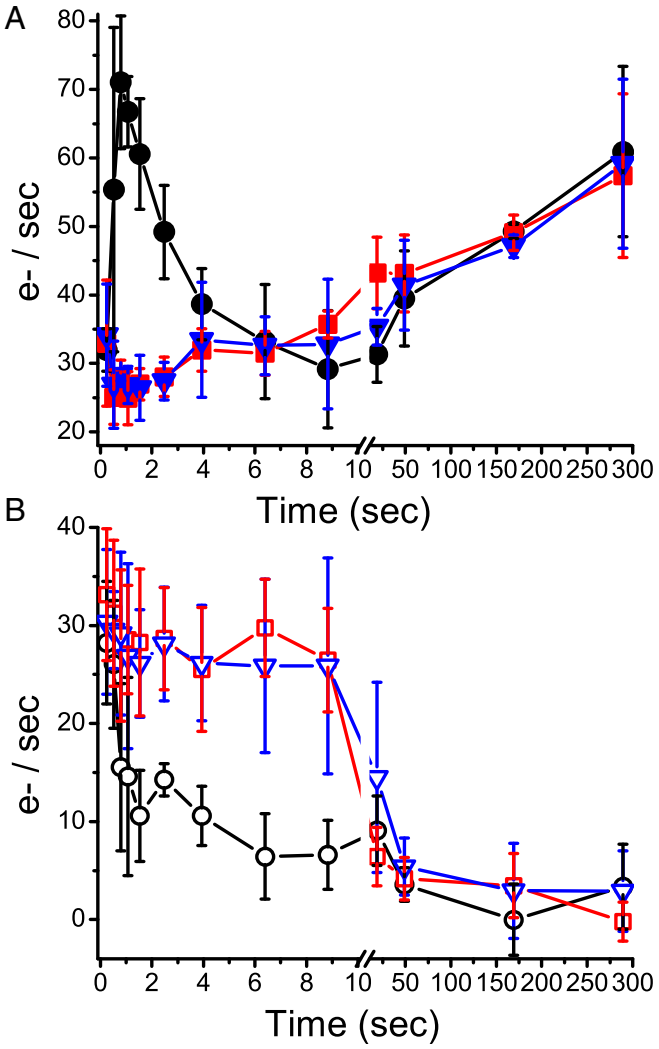

Fig. 2. Photosynthetic electron transport in *P. patens* WT and *flv KO* lines grown in CL. (*A*) Total photosynthetic ETR measured in vivo in WT (black circles), *flva* KO (red squares), and *flvb* KO (blue triangles) at 940 μmol photons $m^{-2}{\cdot}s^{-1}$ actinic light, calculated from electrochromic shift signal, as detailed in *SI Appendix*, Fig. S4. (*B*) Cyclic electron transport rate measured in the same samples treated with the PSII inhibitor DCMU. WT, empty black circles; *flva* KO, empty red squares; *flvb* KO, empty blue triangles. ETR values are normalized to xenon-induced PSI turnovers. Because of the presence of double PSI turnovers using a xenon lamp (24), ETR absolute values are underestimated by ~40% (*SI Appendix*, Fig. S4). Data presented are averages ± SD of three to five independent biological replicates.

PLANT BIOLOGY

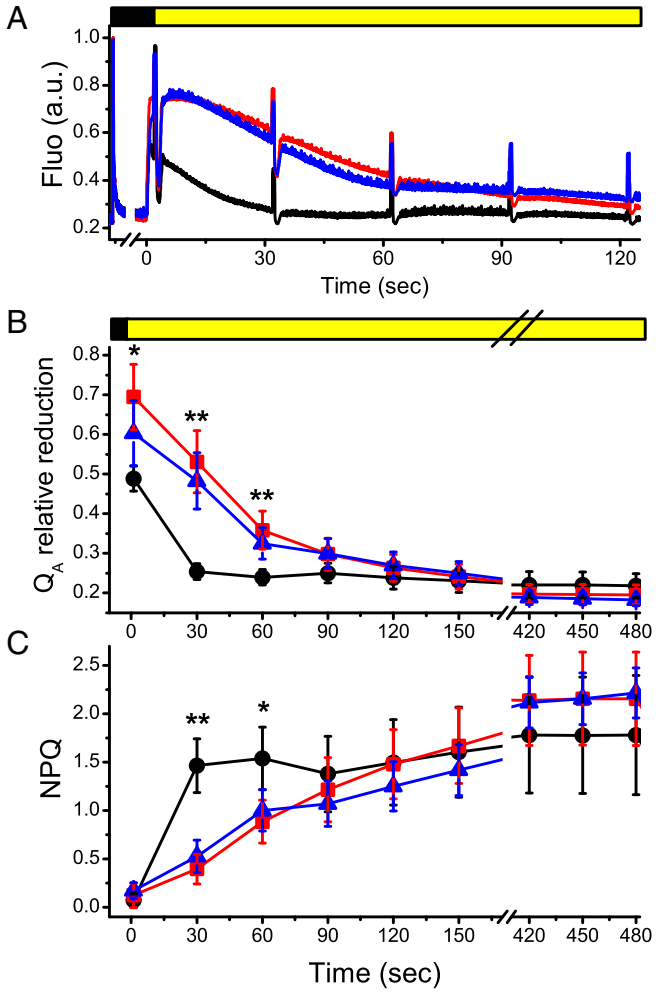

Fig. 3. Evaluation of PSII efficiency in *P. patens flv* KO lines. (*A*) Chl fluorescence kinetics, normalized to the dark acclimated maximum (Fm) value, of WT and *flv* KO lines. A representative kinetic for each genotype is reported (first 120 s after light is switched on). (*B*) Q_A relative reduction and (*C*) heat dissipation of excess energy (NPQ), calculated from fluorescence kinetics (complete measurements are reported in *SI Appendix*, Fig. S7). WT, shown in black; *flva* KO, red; *flvb* KO, blue; all plants were grown 10 d in control light. Upper yellow/black bars indicate when actinic light (175 μmol photons $m^{-2}{\cdot}s^{-1}$) was on/off. Data are reported as average ± SD of four independent biological replicates. Asterisks indicate significant differences between WT and *flv* KOs (*t* test, $*P = 0.05$; $**P = 0.01$).

(Fig. 2*B*). CET activity later decreased, and after 20 s of illumination, its contribution to electron transport in *flv* KO plants became indistinguishable from WT (Fig. 2*B*). Thus, about 1 s after the light was switched on, the major component of electron transport in the WT was FLV-dependent, whereas in *flv* KO mutants the cyclic electron flow was the main pathway activated (*SI Appendix*, Fig. S6).

The effect of FLV depletion was also assessed using chlorophyll (Chl) fluorescence. When dark-acclimated plants are exposed to illumination, Chl fluorescence signal is quenched as a result of the activation of both photosynthetic electron transport and mechanisms dissipating excess excited Chl singlet states as heat (nonphotochemical quenching; NPQ) (28). The induction of this Chl fluorescence quenching on illumination was slower in both *flva* KO and *flvb* KO with respect to WT (Fig. 3*A*). Moreover, both *flva* KO and *flvb* KO showed a higher Q_A redox state in the first few seconds after the light was switched on (Fig. 3*B*), indicating an overreduction of the electron transport chain. Differences between the genotypes gradually disappeared during the illumination period, and all genotypes were indistinguishable after 1 min of light treatment. NPQ induction was also affected in both *flv* KOs, but again, differences with respect to WT were limited to the first minute after the light was switched on (Fig. 3*C*), and WT and *flv* KOs were indistinguishable at steady-state illumination (Fig. 3 and *SI Appendix*, Fig. S7). The same differences in both NPQ and Q_A redox state for the first minute after the light was switched on were present independent from the actinic light intensities used in the analysis (*SI Appendix*, Fig. S8).

PSI efficiency was also monitored in the same experimental conditions, using the $P700^+$ absorption signal (10, 29). In WT plants, when light was switched on, the $P700^+$ signal immediately increased as a result of light-dependent PSI oxidation, then reaching a steady state (Fig. 4*A*). Both *flv* KO genotypes were slower in reaching this steady state, indicating a reduced efficiency in P700 oxidation in the mutants (Fig. 4*A*). Consistently, PSI quantum yield, Y(I), was reduced in *flva* KO and *flvb* KO for the first seconds after the light was switched on (Fig. 4*B*). This was the result of a strong acceptor side limitation in FLV-depleted strains [Y(NA); Fig. 4*C*], whereas both *flv* KO lines showed a smaller donor side limitation [Y(ND)] compared with WT (Fig. 4*D*). The alterations in PSI efficiency were only present in the first seconds after the light was switched on and progressively decreased during illumination (Fig. 4 and *SI Appendix*, Fig. S9). An analogous behavior was observed irrespective of the actinic light intensity used for the measurement, as observed earlier for PSII (*SI Appendix*, Fig. S8). The same analyses were performed in the presence of the artificial electron acceptor methylviologen (30), which, as demonstrated in *SI Appendix*, Fig. S10, rescued the phenotype of the *flv* KO plants, confirming that in these plants, PSI is limited on the acceptor side (*SI Appendix*, Fig. S10).

PSI and PSII functional measurements were also performed treating plants with cycles of dim/saturating actinic light, an

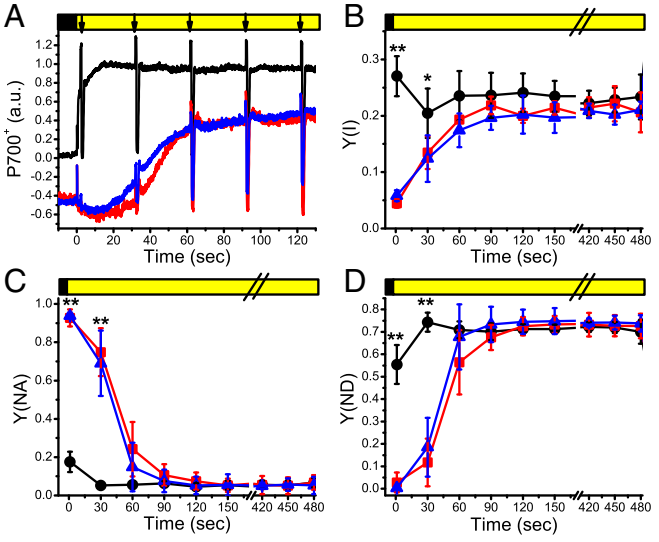

Fig. 4. PSI efficiency in response to illumination. (*A*) Changes in $P700^+$ absorption signal during a dark-to-light transition in WT (black), *flva* KO (red), and *flvb* KO (blue). For each genotype, a representative kinetic is shown. Signals are normalized to the steady state value, and *flva* KO and *flvb* KO kinetics are shifted (–0.5 on the *y* axis) with respect to WT for clarity. Arrows indicate saturation pulses. In *B*, *C*, and *D*, PSI quantum yield of energy conversion [Y(I)], acceptor [Y(NA)], and donor [Y(ND)] side limitation, respectively, are reported as calculated from the $P700^+$ absorption kinetics. Complete kinetics are shown in *SI Appendix*, Fig. S9. WT, black; *flva* KO, red; *flvb* KO, blue; all plants were grown 10 d in control light. Upper yellow/black bars indicate the period where actinic light (540 μmol photons $m^{-2}{\cdot}s^{-1}$) is on/off. Averages ± SD of four independent biological replicates are shown. Asterisks indicate values significantly different between WT and *flv* KOs (*t* test, $*P = 0.05$; $**P = 0.01$).

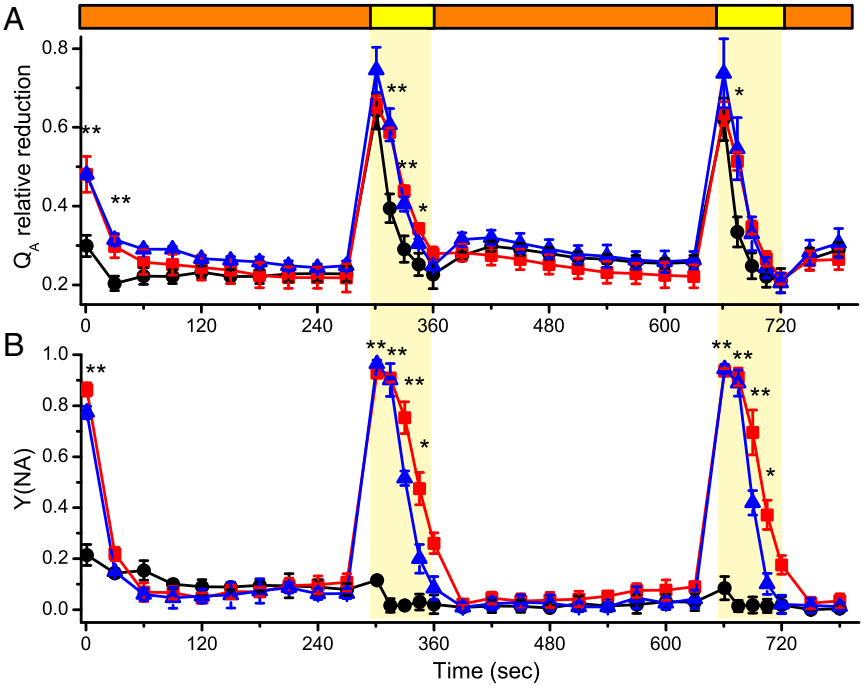

Fig. 5. Effect of FLV depletion on photosystems efficiencies upon light fluctuations. Dark-acclimated moss tissues grown for 10 d in control light were then exposed to cycles of 5 min of mild actinic illumination (50 μmol photons $m^{-2}·s^{-1}$, orange bars) and 1 min strong actinic light (540 μmol photons $m^{-2}·s^{-1}$, yellow bars and shading), monitoring PSII and PSI efficiencies simultaneously. Q_A relative reduction and Y (NA) parameter are reported in *A* and *B*, whereas additional parameters are shown in *SI Appendix*, Fig. S11. WT, *flva* KO, and *flvb* KO lines are shown in black, red, and blue, respectively. Data reported are average ± SD of three independent replicates, and asterisks indicate values significantly different between WT and *flv* KOs (*t* test, $*P = 0.05$; $**P = 0.01$).

illumination regime more representative of a natural environment than a dark-to-light transition (1). PSII and PSI responses observed after each increase in illumination were highly similar to the one detected in the dark-to-light switch presented earlier, with *flv* KOs showing increased relative Q_A reduction (Fig. 5*A*) and strong PSI acceptor side limitation (Fig. 5*B*), together with decreased PSI and PSII yields and a slower NPQ activation (*SI Appendix*, Fig. S11), every time the light intensity increased (yellow shading in Fig. 5 and in *SI Appendix*, Fig. S11).

***flv* KOs Show Increased PSI Photodamage in Fluctuating Light.** Results reported here clearly suggest that the FLV proteins have a significant influence on photosynthetic electron transport during the first seconds after a change in irradiation. To investigate the physiological relevance of this activity in vivo, WT, *flva* KO, and *flvb* KO were grown under a fluctuating light (FL) regime in which plants were treated with recurrent exposition to intense light (1 min at 800 μmol photons $m^{-2}·s^{-1}$ every 6 min). As shown in Fig. 6, in those dynamic light conditions, *flva* KO and *flvb* KO mutants showed a strong reduction in growth with respect to WT. Such a growth phenotype was not present in the case of constant illumination, even of high intensity (Fig. 6). This clearly showed that the *flv* KO mutants are not sensitive to intense irradiation per se but, rather, to fluctuations in light intensity.

When grown under FL conditions, *flva* KO and *flvb* KO plants showed lower PSII efficiency compared with WT (*SI Appendix*, Table S1), but the strongest effect was on PSI, as evidenced by the drastic decrease in PSI/PSII ratio (Fig. 7*A*). *flv* KO mutants treated with FL also showed a strong reduction in maximum $P700^+$ signal (Pm, *SI Appendix*, Table S1), suggesting the altered PSI/PSII ratio was the result of an inactivation of PSI, rather than an increase in PSII. Western blotting analyses consistently showed no significant difference in PSII subunit accumulation between WT and the *flv* KO plants (Fig. 7*B*). Conversely, a decrease in PSI subunits was detected in *flv* KO compared with WT after FL growth (Fig. 7*B*), which further increased when the treatment in FL was prolonged (*SI Appendix*, Fig. S12), suggesting PSI was first inactivated and then slowly degraded. Western blotting with the PGR5 antibody demonstrated, especially in FL conditions, an accumulation of PGR5 in *flv* KO plants (Fig. 7*B*). The PGR5 protein is known to be involved in cyclic electron transport (8).

Discussion

The ability of photosynthetic organisms to convert light into chemical energy requires the generation of pigment excited states and multiple electron transport reactions. This process thus inevitably involves the formation of instable molecules that must be readily consumed to avoid the formation of undesired side products such as reactive oxygen species. As a consequence, all oxygenic photosynthetic organisms must find an optimal compromise between maximizing light use efficiency and maintaining an effective protection from eventual excess of absorbed energy or excited electrons. Keeping such a balance is particularly complex in a highly variable environment in which the energy availability (light) and its use (carbon fixation and metabolism in general) are continuously changing, and it thus requires a constant modulation of photosynthetic efficiency (2, 5, 6, 31–34).

In this article, we demonstrate that in the moss *P. patens*, FLV proteins are active as electron sinks downstream of PSI and are a

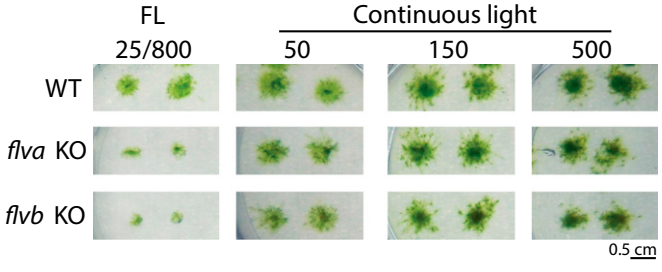

Fig. 6. Growth phenotype of WT and *flv* KO plants in different light conditions. *P. patens* WT, *flva* KO, and *flvb* KO plants were grown for 2 weeks either under constant illumination at 50, 150, or 500 μmol photons $m^{-2}·s^{-1}$, or in fluctuating light (FL, cycles of 5 min at 25 μmol photons $m^{-2}·s^{-1}$ followed by 1 min at 800 μmol photons $m^{-2}·s^{-1}$). It is noteworthy that the FL regime is characterized by the same integrated light intensity as constant illumination at 150 μmol photons $m^{-2}·s^{-1}$.

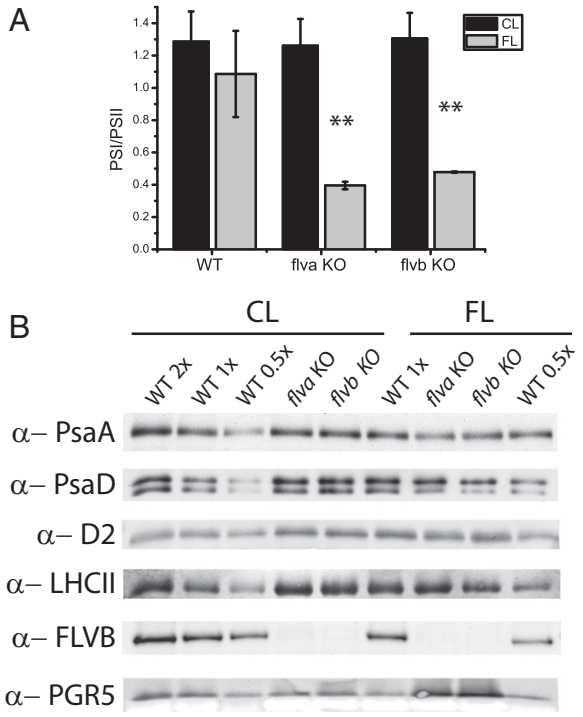

Fig. 7. Long-term effects of fluctuating light on PSI and PSII in *flv* KOs. (*A*) PSI/PSII ratio was determined as detailed in *SI Appendix*, Fig. S4*A* in dark-acclimated plants either grown in constant illumination (CL, 50 μmol photons $m^{-2}{\cdot}s^{-1}$) or in fluctuating light (FL, cycles of 5 min at 25 μmol photons $m^{-2}{\cdot}s^{-1}$, followed by 1 min at 800 μmol photons $m^{-2}{\cdot}s^{-1}$) conditions. PSI content is overestimated because of xenon-induced double turnovers (24), and therefore the PSI/PSII ratios are underestimated by the same extent (~40%). Asterisks (**) indicate values significantly different from WT (*t* test, $P = 0.01$, $n = 3$). (*B*) Western blotting analysis on CL and FL grown plants of WT and *flva* KO and *flvb* KO using antibodies against FLVB, PGR5, PSI (PsaA and PsaD), and PSII (D2 and LHCII) subunits. Whereas 0.5 Chl μg thylakoid extracts were used for LHCII and 1 Chl μg thylakoid extracts for all of the other cases, 5 Chl μg total protein extracts were loaded for each sample for FLVB, 4 Chl μg for PGR5 immunodetection. For WT, 0.5X and 2X indicates lane loaded with half or double those Chl μg amounts, respectively.

major component of the photosynthesis regulation machinery, with a seminal role in fluctuating light conditions. FLV activity is prominent for a few seconds after an increase in illumination, being responsible for a transient peak in ETR of WT plants, which is completely missing from the *flv* KO mutants (Fig. 2*A*). This reduction in electron transport ability in *flv* KO caused a strong acceptor side limitation in PSI (Figs. 4 and 5) and over-reduction of electron transporters (Figs. 3 and 5) after any increase in illumination. FLV effect on electron transport is, however, transient and after 1 min of light exposure, all of the effects on PSI, Q_A redox state, or ETR are absent, making the *flv* KO mutants and WT indistinguishable. This observation suggests that during prolonged illumination with various constant light intensities, the role of FLVs role is negligible, and other metabolic pathways (e.g., carbon fixation reactions) consume the NADPH/ATP produced, therefore protecting the photosynthetic chain from over-reduction in steady state illumination, even in the presence of strong light (Fig. 6).

The biological significance for this transient, FLV-dependent increase in ETR on a sudden increase in light intensity is in accordance with the general knowledge that light absorption and electron transfer are immediately affected by any change in illumination conditions. In contrast, regulation of metabolism and carbon fixation have slower kinetics, and thus they are not immediately capable of consuming all the ATP and reducing power produced, generating a dangerous imbalance between production of excited states and consumption of the final products of photosynthetic electron transport. FLV proteins, in accepting electrons from PSI (Fig. 2), consume a significant fraction of the extra reducing power available, and thus avoid over-reduction of electron transport chain. In this context, it should also be considered that oxidized P700 ($P700^+$) is a very good quencher of Chl excited states (35–38). PSI is tolerant to excess excitation energy, being able to induce nonphotochemical energy dissipation even when damaged (39), but instead it is extremely sensitive to excess electrons on the donor side of the complex (36, 37). In WT, FLV activity as electron sink maintains PSI in a donor state limitation (Fig. 4*D* and *SI Appendix*, Fig. S9), thus keeping it in a more stable state, effectively protecting it from light-induced damage as a result of excess electrons. Conversely, in *flv* KO mutants, PSI activity is not limited at the donor side (Fig. 4*D* and *SI Appendix*, Fig. S9), and the resulting electron pressure toward PSI caused the drastic PSI inactivation in *flv* KOs (Fig. 7 and *SI Appendix*, Table S1).

An additional beneficiary effect of FLV activity is a result of its contribution to the total electron transport (Fig. 2) that supports proton translocation into the lumen, as confirmed by the observation that *flv* KO mutants show an alteration of total transmembrane potential and ΔpH formation (*SI Appendix*, Fig. S13). Lumen acidification is well known to be a major signal for the activation of several photo-protection mechanisms such as NPQ, xanthophyll cycle, and cytb_6f regulation (6, 32, 33, 40–42). FLV activity thus allows for a faster activation of these mechanisms (Fig. 3), leading to a decreased excitation pressure by activation of heat dissipation of excess absorbed energy, and thus contributing to protection of whole photosynthetic apparatus, including PSII (*SI Appendix*, Table S1). The biological relevance of FLV activity is well visualized when plants are exposed to a fluctuating light regime, conditions in which its activity is continuously required. FLV-depleted mutants show strong growth defects and PSI photodamage (Figs. 6 and 7), whereas an even stronger illumination does not affect FLV mutants if provided constantly (Fig. 6).

Considering such a strong effect on photosynthesis regulation, it is surprising that FLVs are not conserved in angiosperms (3, 12, 16, 19). A recent report showed that FLVs from *P. patens* are capable of accepting electrons from PSI when expressed in *A. thaliana* (19), and thus this loss was not a result of mechanistic or structural reasons but, rather, to a change in regulatory strategies that made FLV activity superfluous or even detrimental. A likely explanation can be found by observing that in *flv* KO mutants, cyclic electron transport partially compensates for the absence of FLV (Figs. 2 and 7*B*), clearly suggesting CET could have taken over the FLV function in protecting PSI from over-reduction in plants. This hypothesis is consistent with the observations that CET is transiently activated on dark-to-light transitions in vascular plants (6, 26), and that *A. thaliana* CET mutants also show PSI photosensitivity when exposed to light fluctuations (8, 29).

Materials and Methods

Plant Material and Light Treatments. Protonemal tissue of *P. patens*, Gransden WT strain, *flva* and *flvb* single KO lines were grown on minimum $PpNO_3$ media in controlled conditions: 24 °C, 16 h light/8 h dark photoperiod and a light intensity of 50 μmol photons $m^{-2}{\cdot}s^{-1}$ (control light, CL), and analyzed after 10 d of growth. For fluctuating light treatment (FL), 3-d-old plates grown in CL were moved to a light regime with cycles of 5 min at 25 μmol photons $m^{-2}{\cdot}s^{-1}$ and 1 min at 800 μmol photons $m^{-2}{\cdot}s^{-1}$ during the light phase of photoperiod and analyzed after 7 d in FL (10-d-old plates).

The growth phenotype of *flv* KO lines was evaluated on spots of tissue grown in different constant light intensities [50 (CL), 150, or 500 μmol photons $m^{-2}{\cdot}s^{-1}$], or FL. It should be mentioned that the plants grown at 150 μmol photons $m^{-2}{\cdot}s^{-1}$ received almost the same total amount of photons of FL conditions.

***flva* and *flvb* KO Constructs Design, Moss Transformation, and Screening of Resistant Lines.** Selected upstream and downstream homologous recombination regions from *FLVA* (locus XP_001759251.1) and *FLVB* (XP_001756079.1) genes were

amplified by PCR from WT genomic DNA and cloned respectively into BHRf and BNRf plasmids (kindly provided by F. Nogue, INRA Versailles, France), for targeted KO generation of *FLVA* or *FLVB* genes, respectively, as detailed in *SI Appendix*, Table S2 and Fig. S2*A*.

WT Gransden strain was then used as genetic background to obtain *flva* KO and *flvb* KO single KO lines. *P. patens* transformation was performed as in ref. 20, with minor modifications (21). After two rounds of selection, genomic DNA from WT and resistant lines was obtained with EuroGOLD Plant DNA mini kit (EuroClone) and used as templates to confirm DNA insertion by PCR (see *SI Appendix*, Table S2 for the primers list). RNA was afterward purified with RNeasy Plant Mini Kit (Qiagen) and used as a template for cDNA synthesis with RevertAid Reverse Transcriptase (Thermo Scientific) to verify *FLVA/B* gene expression in WT, *flva* KO, and *flvb* KO.

Thylakoid and Total Protein Extracts. Thylakoids from protonemal tissue grown in CL or FL were prepared by means of an *Arabidopsis* protocol with minor modifications, as in ref. 43. Total extracts were instead obtained by grinding tissues in sample buffer before SDS/PAGE. For immunoblotting analysis, after SDS/PAGE, proteins were transferred to nitro-cellulose membranes (Pall Corporation) and detected with specific commercial (anti-PsaA and anti-PsaD, Agrisera, catalog numbers AS06 172 and AS09 461, respectively), custom-made (anti-FLVA, anti-FLVB and anti-PGR5, from Agrisera) or homemade polyclonal antibodies (D2 and LHCII). Chl a/b and Chl/Car ratios were obtained by fitting the spectrum of 80% acetone pigment extracts with spectra of the individual purified pigments, as in ref. 44.

Fluorescence and P700 Measurement with Dual-PAM. In vivo chlorophyll fluorescence and oxidized $P700^+$ absorption signal were monitored simultaneously at room temperature with a Dual PAM-100 fluorometer (Walz) in *P. patens* WT, *flva* KO, and *flvb* KO tissues grown for 10 d in minimum medium ($PpNO_3$) in control growth conditions (CL). Before measurements, plates were dark-acclimated for 40 min. For induction/recovery kinetics, actinic light was set to 540 (saturating actinic light), 175, or 50 μmol photons $m^{-2}{\cdot}s^{-1}$. For fluctuating light mimicking kinetics, actinic light was set at 50 μmol photons $m^{-2}{\cdot}s^{-1}$ for mild illumination and 540 μmol $m^{-2}{\cdot}s^{-1}$ for the saturating light steps. PSII and PSI parameters were calculated as following: Fv/Fm as (Fm − Fo)/Fm, Y(II) as (Fm′ − F)/Fm′, relative Q_A reduction as F′/Fm, NPQ as (Fm − Fm′)/Fm′, Y(I) as 1 − Y(ND) − Y(NA), Y(NA) as (Pm − Pm′)/Pm, Y(ND) as (1 − P700 red). Data are presented as mean ± SD of at least 3 independent experiments.

Spectroscopic Analyses with Joliot-Type Spectrometer (JTS). Spectroscopic analysis on WT, *flva* KO and *flvb* KO lines was performed in vivo on 10-d-old intact tissues, using a JTS-10 spectrophotometer (Biologic). Relative amount of functional photosynthetic complexes and electron transport rates were evaluated measuring the electrochromic shift spectral change, using a protocol already used in refs. 22, 24–26 as detailed in *SI Appendix*, Fig. S4.

ACKNOWLEDGMENTS. C.G. acknowledges financial support by the University of Padova (Grant GRIC13V6YZ) and by the Ingegner Aldo Gini Foundation (Padova). T.M. received financial support from the European Research Council (BIOLEAP Grant 309485), and E.-M.A. received financial support from the Academy of Finland (Grants 271832 and 273870).

1. Külheim C, Agren J, Jansson S (2002) Rapid regulation of light harvesting and plant fitness in the field. *Science* 297(5578):91–93.
2. Allahverdiyeva Y, Suorsa M, Tikkanen M, Aro EM (2015) Photoprotection of photosystems in fluctuating light intensities. *J Exp Bot* 66(9):2427–2436.
3. Peltier G, Tolleter D, Billon E, Cournac L (2010) Auxiliary electron transport pathways in chloroplasts of microalgae. *Photosynth Res* 106(1-2):19–31.
4. Arnon DI, Chain RK (1975) Regulation of ferredoxin-catalyzed photosynthetic phosphorylations. *Proc Natl Acad Sci USA* 72(12):4961–4965.
5. Shikanai T (2014) Central role of cyclic electron transport around photosystem I in the regulation of photosynthesis. *Curr Opin Biotechnol* 26:25–30.
6. Joliot P, Johnson GN (2011) Regulation of cyclic and linear electron flow in higher plants. *Proc Natl Acad Sci USA* 108(32):13317–13322.
7. Peltier G, Aro EM, Shikanai T (2016) NDH-1 and NDH-2 plastoquinone reductases in oxygenic photosynthesis. *Annu Rev Plant Biol* 67:55–80.
8. Munekage Y, et al. (2002) PGR5 is involved in cyclic electron flow around photosystem I and is essential for photoprotection in Arabidopsis. *Cell* 110(3):361–371.
9. Peng L, Fukao Y, Fujiwara M, Takami T, Shikanai T (2009) Efficient operation of NAD(P)H dehydrogenase requires supercomplex formation with photosystem I via minor LHCI in Arabidopsis. *Plant Cell* 21(11):3623–3640.
10. Allahverdiyeva Y, et al. (2013) Flavodiiron proteins Flv1 and Flv3 enable cyanobacterial growth and photosynthesis under fluctuating light. *Proc Natl Acad Sci USA* 110(10):4111–4116.
11. Helman Y, et al. (2003) Genes encoding A-type flavoproteins are essential for photoreduction of O2 in cyanobacteria. *Curr Biol* 13(3):230–235.
12. Allahverdiyeva Y, Isojärvi J, Zhang P, Aro E-M (2015) Cyanobacterial oxygenic photosynthesis is protected by Flavodiiron proteins. *Life (Basel)* 5(1):716–743.
13. Vicente JB, Carrondo MA, Teixeira M, Frazão C (2008) Structural studies on flavodiiron proteins. *Methods Enzymol* 437:3–19.
14. Zhang P, et al. (2012) Operon flv4-flv2 provides cyanobacterial photosystem II with flexibility of electron transfer. *Plant Cell* 24(5):1952–1971.
15. Bersanini L, et al. (2014) Flavodiiron protein Flv2/Flv4-related photoprotective mechanism dissipates excitation pressure of PSII in cooperation with phycobilisomes in Cyanobacteria. *Plant Physiol* 164(2):805–818.
16. Zhang P, Allahverdiyeva Y, Eisenhut M, Aro E-M (2009) Flavodiiron proteins in oxygenic photosynthetic organisms: Photoprotection of photosystem II by Flv2 and Flv4 in Synechocystis sp. PCC 6803. *PLoS One* 4(4):e5331.
17. Jokel M, et al. (2015) Chlamydomonas Flavodiiron proteins facilitate acclimation to anoxia during sulfur deprivation. *Plant Cell Physiol* 56(8):1598–1607.
18. Dang K-V, et al. (2014) Combined increases in mitochondrial cooperation and oxygen photoreduction compensate for deficiency in cyclic electron flow in Chlamydomonas reinhardtii. *Plant Cell* 26(7):3036–3050.
19. Yamamoto H, Takahashi S, Badger MR, Shikanai T (2016) Artificial remodelling of alternative electron flow by Flavodiiron proteins in Arabidopsis. *Nat Plants* 2(3):16012.
20. Schaefer DG, Zrÿd JP (1997) Efficient gene targeting in the moss Physcomitrella patens. *Plant J* 11(6):1195–1206.
21. Alboresi A, Gerotto C, Giacometti GM, Bassi R, Morosinotto T (2010) Physcomitrella patens mutants affected on heat dissipation clarify the evolution of photoprotection mechanisms upon land colonization. *Proc Natl Acad Sci USA* 107(24):11128–11133.
22. Allorent G, et al. (2015) Adjustments of embryonic photosynthetic activity modulate seed fitness in Arabidopsis thaliana. *New Phytol* 205(2):707–719.
23. Kukuczka B, et al. (2014) Proton gradient regulation5-like1-mediated cyclic electron flow is crucial for acclimation to anoxia and complementary to nonphotochemical quenching in stress adaptation. *Plant Physiol* 165(4):1604–1617.
24. Bailleul B, Cardol P, Breyton C, Finazzi G (2010) Electrochromism: A useful probe to study algal photosynthesis. *Photosynth Res* 106(1-2):179–189.
25. Joliot P, Joliot A (2002) Cyclic electron transfer in plant leaf. *Proc Natl Acad Sci USA* 99(15):10209–10214.
26. Joliot P, Béal D, Joliot A (2004) Cyclic electron flow under saturating excitation of dark-adapted Arabidopsis leaves. *Biochim Biophys Acta* 1656(2-3):166–176.
27. Bendall DS, Manasse RS (1995) Cyclic photophosphorylation and electron transport. *Biochim Biophys Acta - Bioenerg* 1229(1):23–38.
28. Baker NR (2008) Chlorophyll fluorescence: A probe of photosynthesis in vivo. *Annu Rev Plant Biol* 59:89–113.
29. Suorsa M, et al. (2012) PROTON GRADIENT REGULATION5 is essential for proper acclimation of Arabidopsis photosystem I to naturally and artificially fluctuating light conditions. *Plant Cell* 24(7):2934–2948.
30. Schansker G, Tòth SZ, Strasser RJ (2005) Methylviologen and dibromothymoquinone treatments of pea leaves reveal the role of photosystem I in the Chl a fluorescence rise OJIP. *Biochim Biophys Acta - Bioenerg* 1706(3):250–261.
31. Rochaix J-D (2014) Regulation and dynamics of the light-harvesting system. *Annu Rev Plant Biol* 65:287–309.
32. Li Z, Wakao S, Fischer BB, Niyogi KK (2009) Sensing and responding to excess light. *Annu Rev Plant Biol* 60:239–260.
33. Niyogi KK, Truong TB (2013) Evolution of flexible non-photochemical quenching mechanisms that regulate light harvesting in oxygenic photosynthesis. *Curr Opin Plant Biol* 16(3):307–314.
34. Tikkanen M, Aro E-M (2014) Integrative regulatory network of plant thylakoid energy transduction. *Trends Plant Sci* 19(1):10–17.
35. Shubin VV, Terekhova IN, Kirillov BA, Karapetyan NV (2008) Quantum yield of P700+ photodestruction in isolated photosystem I complexes of the cyanobacterium Arthrospira platensis. *Photochem Photobiol Sci* 7(8):956–962.
36. Sonoike K (2011) Photoinhibition of photosystem I. *Physiol Plant* 142(1):56–64.
37. Chaux F, Peltier G, Johnson X (2015) A security network in PSI photoprotection: Regulation of photosynthetic control, NPQ and O2 photoreduction by cyclic electron flow. *Front Plant Sci* 6:875.
38. Caffarri S, Tibiletti T, Jennings RC, Santabarbara S (2014) A comparison between plant photosystem I and photosystem II architecture and functioning. *Curr Protein Pept Sci* 15(4):296–331.
39. Tiwari A, et al. (2016) Photodamage of iron–sulphur clusters in photosystem I induces non-photochemical energy dissipation. *Nat Plants* 2(4):16035.
40. Niyogi KK, Grossman AR, Björkman O (1998) Arabidopsis mutants define a central role for the xanthophyll cycle in the regulation of photosynthetic energy conversion. *Plant Cell* 10(7):1121–1134.
41. Li XP, et al. (2000) A pigment-binding protein essential for regulation of photosynthetic light harvesting. *Nature* 403(6768):391–395.
42. Foyer CH, Neukermans J, Queval G, Noctor G, Harbinson J (2012) Photosynthetic control of electron transport and the regulation of gene expression. *J Exp Bot* 63(4):1637–1661.
43. Gerotto C, Alboresi A, Giacometti GM, Bassi R, Morosinotto T (2012) Coexistence of plant and algal energy dissipation mechanisms in the moss Physcomitrella patens. *New Phytol* 196(3):763–773.
44. Croce R, Canino G, Ros F, Bassi R (2002) Chromophore organization in the higher-plant photosystem II antenna protein CP26. *Biochemistry* 41(23):7334–7343.